Gemini Near-IR Integral Field Spectroscopy of the central region of Mrk1066

Rogemar A. Riffel[1,2] & Thaisa Storchi-Bergmann[2]

[1]Departamento de Física – CCNE/UFSM; [2]Departamento de Astronomia – IF/UFRGS

Introduction

We present results from Integral Field Spectroscopy in the J and K bands of the inner 700 pc of the Seyfert 2 galaxy Mrk 1066 at a spatial resoluton of ~25 pc (0.12") obtained with the Gemini's Near-infrared Integral Field Spectrograph (NIFS) operating with the ALTAIR adaptive optics module.

Mrk 1066 is an inclinated SB0+ galaxy located at a distance of 48 Mpc, which yields a spatial scale of 234 pc arcsec^{-1}. This galaxy presents a jetlike feature in [OIII]+Hβ HST narrow band image which extends to 1.4" NW from the nucleus, while the Hα+[NII] emission is extended to both sides of the nucleus along the position angle PA~130^0 (Bower et al. 1995). The 3.6 cm radio emission is well aligned with the optical emission-line structure (Nagar et al. 1999).

Results and Discussion

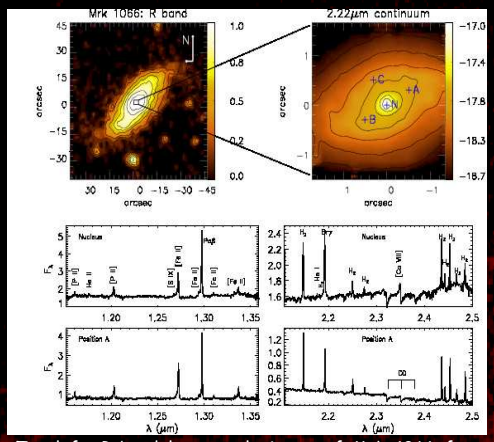

Top left: R-band large scale image of Mrk 1066 from Lasker et al. (1996). The central box shows the IFU field of view. Top right: K-band continuum image from NIFS spectroscopy. Bottom: J and K band spectra for the positions N and A marked at the continuum image for an aperture of 0.25"x0.25". The emission lines used to study the gaseous distribution and kinematics are identified in the nuclear spectrum, while the CO bandheads used to obtain the stellar kinematics are identified in the extra-nuclear spectrum.

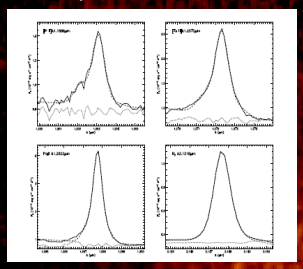

Sample of Gauss-Hermite series fits of the emission-line profiles at 0.5" NW from the nucleus. The resulting fit is shown as dashed lines and the observed profiles as continuum lines.

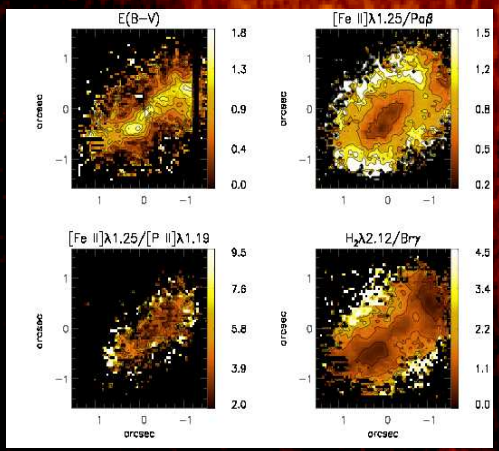

Line-ratio maps constructed in order to invertigate the extinction and excitation of the Narrow Line Region of Mrk 1066. The reddening map was obtained from the Brγ/Paβ intensity ratio.

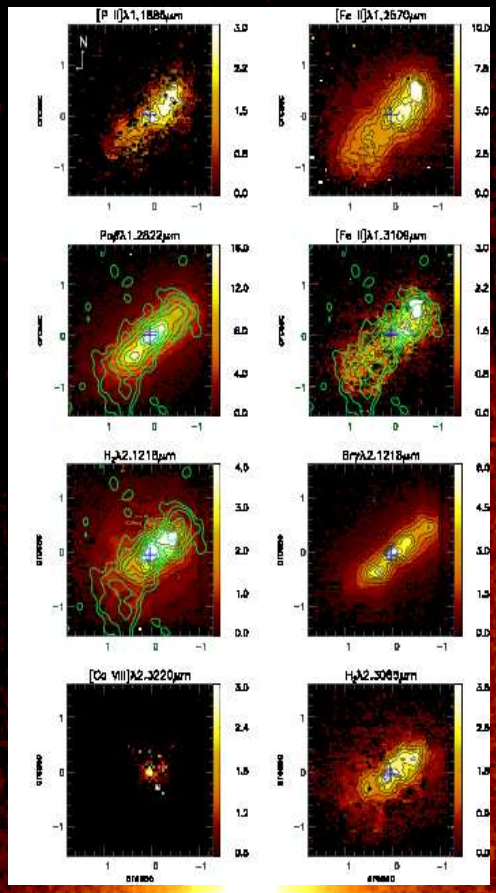

Emission-line flux distributions obtained from the fitting of the emission-line profiles. The green contours overlaied to Paβ, [FeII]λ1.31μm and H$_2$λ2.12μm maps are from the 3.6 cm radio image from Nagar et al. (1999). The flux scale is in 10^{-17} erg cm^{-2}s^{-1}. Extended emission up to 1.4" (~330 pc) from the nucleus is observed in all lines (with exception of the [CaVIII] line, which is not resolved by our observations). The peak fluxes of [PII] and [FeII] emission occur at ~0.85" NW from the nucleus, approximately at the same location where is observed a hotspot at the radio emission. The H recombination lines peak at the nucleus and present a secondary peak at ~0.5" SE from the nuclues. The H$_2$ flux distribution also peaks at the nucleus and is more uniformly distributed in the whole IFU field than the other emission lines.

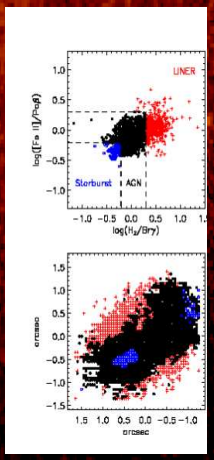

Line-ratio diagnostic diagram (Larkin et al. 1998; Rodríguez-Ardila, 2004, 2005) . Mrk 1066 present a typical Seyfert spectra at positions along the radio jet. At positions away from it the H$_2$/Brγ ratio is enhanced, probably due to additional H$_2$ emission from X-ray heated gas. At ~0.5" SE from the nuclues there is a region typical of Starburst emission. This region is coincident with the secondary peak flux observed in the H recombination lines, indicating the presence of star formation at this location.

Excitation: Using models of Malloney, Hollembach & Tielens (1996) to calculate the predicted emission of the [FeII] and H$_2$ lines from X-ray heated gas we conclude that X-rays can account for only 25% of the H$_2$ observed emission and even less for the [FeII] emission. From this analisys, together with the correlation observed between the line and radio emissions and analysis of the emission-line intensity ratios, we conclude that shocks produced by the radio jet are the dominant excitation mechanism of the H$_2$ lines, while the [FeII] has an additional emission due to photoionization.

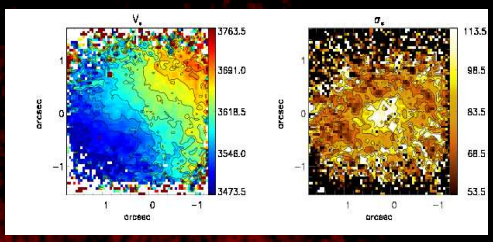

Stellar kinematics obtained by fitting the CO absorption bandhead in the K-band by stellar templates from Winge et al (2009) using the pPXF technique (Cappellari & Emsellem 2004). The stellar velocity field is dominated by rotation and the velocity dispersion map shows a circumnuclear ring of lower σ values (~80 km s^{-1}) immersed in the dispersion of the stars of the bulge (σ~110 km s^{-1}).

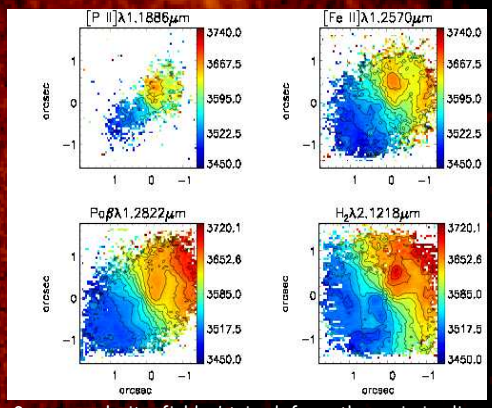

Gaseous velocity field obtained from the emission-line profiles. The velocity fields present additional components when compared to the stellar velocity field and are distinct for each emission line.

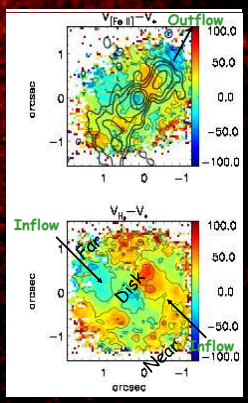

Residual maps between gaseous and stellar velocity fields showing that the H$_2$ and [FeII] emitting gas have distinct kinematics. The H$_2$ (bottom panel) presents a small disk (~180 pc) surrounding the nucleus. Probably this disk is feeded by inflows of gas along the spiral structures observed in blueshifts in the far side of the galaxy (NE) and in redshifts in the near side (SW), as indicated in the figure. The [FeII] (top panel) presents an additional outflow near the edge of the radio jet, indicating the interaction between the jet and the [FeII] emitting gas.

Main Conclusions

- The stellar velocity field is dominated by rotation and the velocity dispersion map shows a circumnuclear ring of lower σ values immersed in the dispersion of the bulge stars.
- The H$_2$ flux distribution is dominated by emission due to excitation by shocks produced by the radio jet, while the [FeII] has an additional emission from photoionized gas.
- H$_2$ and [FeII] present distinct kinematics and flux distributions. The former present a small rotating disk and inflowing gas along spiral arms, suggesting that the H$_2$ traces the feeding of the AGN, while the [FeII] has an additional outflowing component with velocity of ~70 km s^{-1} near the edge of the radio jet. This result is in good agreement with previos results from IFU spectroscopy for other Seyfert galaxies (e.g. Riffel et al. 2006, 2008, 2009, Storchi-Bergmann et al. 2009).

References

Cappellari & Emsellem, 2004, PASP, 116, 138.
Larkin et al., 1998, ApJS, 114, 59.
Lasker et al., 1996, ASP Conference Series, 101, 88.
Rodríguez-Ardila et al, 2004, A&A, 425, 457.
Rodríguez-Ardila et al, 2005, MNRAS, 364, 1041.
Maloney, Hollembach & Tielens, 1996, ApJ 466, 561.
Nagar et al., 1999, ApJS, 120, 209.
Riffel at al., 2006, MNRAS, 371, 170.
Riffel et al., 2008, MNRAS, 385, 1129.
Riffel et al., 2009, MNRAS, 393, 783.
Storchi-Bergmann et al., 2009, MNRAS, 394, 1148.
Winge, Riffel & Storchi-Bergmann, 2009, ApJS, 185, 186.